Detection of quantum critical points by a probe qubit [*]

Jingfu Zhang, Xinhua Peng, Nageswaran Rajendran, and Dieter Suter

Technische Universität Dortmund,

44221 Dortmund, Germany

(Dated: March 14, 2008)

Abstract

Quantum phase transitions occur when the ground state of a quantum system undergoes a qualitative change when an external control parameter reaches a critical value. Here, we demonstrate a technique for studying quantum systems undergoing a phase transition by coupling the system to a probe qubit. It uses directly the increased sensibility of the quantum system to perturbations when it is close to a critical point. Using an NMR quantum simulator, we demonstrate this measurement technique for two different types of quantum phase transitions in an Ising spin chain.

PACS numbers: 03.67.Lx, 73.43.Nq

[*] Corresponding authors: Jingfu Zhang, zhangjfu2000@yahoo.com;
Dieter Suter, Dieter.Suter@uni-dortmund.de

Introduction.— Phase transitions describe sudden changes in the properties of a physical system when an external control parameter changes through some critical value. If the system under consideration is a quantum mechanical system in its ground state, i.e. at zero temperature, and the phase transition occurs as a function of a non-thermal control parameter, we speak of quantum phase transitions (QPTs) [1]. Examples include the transitions in superconductors [2] and fractional quantum Hall systems [3]. Related phenomena have also been experimentally observed in heavy Fermion systems [4], common metals [5], and in Bose-Einstein condensates [6]. QPTs occur as a result of competing interactions and the different phases often show different types of correlations between the constituents, with correlation lengths that can become arbitrarily large. When specific quantum effects of phase transitions are of interest, it is therefore natural to compare entanglement in the different phases [7, 8].

Experimental observations of QPTs are relatively straightforward when they are accompanied by a change of a suitable order parameter, such as the conductivity or susceptibility in superconductors or the total magnetization in some spin chains [7, 9]. However, such global measurements cannot provide all the details and they are not suitable for closer investigations of the systems in the interesting area close to the critical points. Moreover, not all order parameters can be measured by global measurements. A complete analysis of the system is provided by quantum state tomography [9, 10], but this approach scales very poorly with the size of the system.

As a possible alternative for closer investigations of quantum systems in the vicinity of critical points, it was suggested to compare the evolution of systems at slightly different values of the control parameter. This approach may be considered as a visualization of "quantum fluctuations". Different possibilities exist for comparing these evolutions, some of which have been called Loschmidt echo (LE) or fidelity decay [11]. In the vicinity of critical points, the systems are expected to be much more susceptible to external perturbations than in the center of a phase [12]. Such a comparison is possible by coupling the system under study to a second quantum system, consisting in the simplest case of a single qubit. The two states of the probe qubit can then be used to probe the system under two different values of the control parameter. The signal obtained in this case corresponds to the overlap of two states evolving under slightly different control parameters.

In this Letter we implement this protocol in a nuclear magnetic resonance (NMR) quan-

tum information processor. The system undergoing the QPT corresponds to an Ising-type spin chain and the control parameter to a longitudinal magnetic field. In a purely longitudinal field, the ground state is degenerate at the critical points. This degeneracy is lifted if the magnetic field contains a transverse component. For the longitudinal as well as for the transverse case, we measure the QPT by coupling the spin chain to a probe qubit.

Level-crossing.— We first consider a QPT in the Ising model in a minimal system consisting of two spins $1/2$. Its Hamiltonian is

$$H^s = \sigma_z^1 \sigma_z^2 + B_z(\sigma_z^1 + \sigma_z^2), \tag{1}$$

where the σ_z^i are Pauli operators and B_z is a magnetic field. The units have been chosen such that the coupling constant between the two qubits is 1. For the purpose of this paper, it is sufficient to consider the triplet manyfold. Within this subsystem, the ground state depends on the field strength:

$$|\psi_g(B_z)\rangle = \begin{cases} |00\rangle & (B_z \leq -1) \\ |\phi^+\rangle & (-1 \leq B_z \leq 1) \\ |11\rangle & (B_z \geq 1), \end{cases} \tag{2}$$

where $|\phi^+\rangle = (|01\rangle + |10\rangle)/\sqrt{2}$. Figure 1 shows the energy levels of the system and the concurrence of the ground state. Obviously $B_z = \pm 1$ are the critical points. The low-field phase is maximally entangled ($C = 1$), while the high-field phases correspond to product states ($C = 0$).

In this system, the QPTs occur at points where the ground state is degenerate. Close to this critical point, it is therefore very susceptible to small perturbations. If we couple it to a probe qubit (which we label 0) via the interaction $\varepsilon\sigma_z^0(\sigma_z^1 + \sigma_z^2)$, the total (three-qubit) system can be decomposed into two subsystems, in which qubits 1 and 2 "see" an effective field $B_z \pm \varepsilon$. If these two fields fall on different sides of the critical point, the "state overlap" [13] $L = |\langle \psi_g(B_{z,0})|\psi_g(B_{z,1})\rangle|^2$ vanishes, otherwise it is unity, as shown by the thin line in Figure 1. Here, $B_{z,0} = B_z + \varepsilon$ specifies the effective field for the subsystem coupled to $|0\rangle_0$ and correspondingly for the other subsystem. In the extreme case where the two states of the probe qubit are orthogonal ($L = 0$), the probe qubit has "measured" the quantum system [14].

To measure L, we first initialize the system and probe qubits into the ground state $|000\rangle$. From there a Walsh-Hadamard transform places the probe qubit into the symmetric

superposition state $|+\rangle = (|0\rangle+|1\rangle)/\sqrt{2}$. We then use the interaction between the probe and the system to apply a conditional evolution to the two system qubits 1 and 2: if the probe qubit is in state $|0\rangle$, the system evolves from $|00\rangle \rightarrow |\psi_g(B_{z,0})\rangle$, and if qubit 0 is in state $|1\rangle$, the system evolves from $|00\rangle \rightarrow |\psi_g(B_{z,1})\rangle$. The network representation of this process is shown in Figure 2(a) [15]. P_0 and P_1 denote the conditional evolutions. The output of the network is

$$|\Psi\rangle = [|0\rangle|\psi_g(B_{z,0})\rangle + |1\rangle|\psi_g(B_{z,1})\rangle]/\sqrt{2}. \tag{3}$$

Taking the trace over the (12)-system, one obtains the reduced density matrix $\rho^{(0)}$ of the probe qubit. The off-diagonal elements are $\rho_{12}^{(0)} = \rho_{21}^{(0)\dagger} = \langle\psi_g(B_{z,0})|\psi_g(B_{z,1})\rangle$. Hence the overlap L can be obtained by measuring $L = 4|\langle\sigma_+^0\rangle|^2$, the transverse magnetization of the probe qubit, which can be observed as a free induction decay.

For the experimental implementation, we chose the nuclear spins of ^{13}C, ^{1}H, and ^{19}F of Diethyl-fluoromalonate as qubits, shown in Figure 2(b). The scalar coupling constants are $J_{12} = 47.6$ Hz, $J_{10} = 161.3$ Hz and $J_{20} = -192.2$ Hz. The sample consisted of a 2.3:1 mixture of unlabeled Diethyl fluoromalonate and d6-acetone. Molecules with a ^{13}C nucleus, which we used as the quantum register, were therefore present at a concentration of about 0.7%.

The effective pure state $|000\rangle$ was prepared by spatial averaging [16]. We implemented the quantum network of Figure 2(a) for five cases corresponding to $B_z = -1.5$, -1, 0, 1, 1.5, respectively. As an example, Figure 2(c) shows the pulse sequence when $B_z = -1$. Figure 3 shows the experimental results. The spectra on top were measured for the values of $B_z = -1.5$, 0, and $+1$, and the asterisks indicate the integrated signal amplitudes. Clearly, the integrated signal essentially vanishes at the quantum critical point, while it remains close to the maximum inside the three phases, in excellent agreement with the theoretical expectation.

Avoided level-crossing.— If we add a transverse field to the system, the QPTs are no longer singular points, but they acquire a finite width. The modified Hamiltonian is

$$H_T^s = \sigma_z^1\sigma_z^2 + B_x(\sigma_x^1 + \sigma_x^2) + B_z(\sigma_z^1 + \sigma_z^2). \tag{4}$$

As long as $B_x \ll 1$, the ground states are very close to those of Eq. (2), except in the vicinity of the critical points, where the transverse field mixes them, thus avoiding the level crossing. In this region, it is sufficient to consider the two lowest energy states. They form

4

a two-level system that can be described by the effective Hamiltonian

$$H_{eff} = -|B_z|I + (1 - |B_z|)\sigma_z + \sqrt{2}B_x\sigma_x,$$

where I denotes the unit operator. Within this approximation, the ground state is $|\psi_g(B_x, B_z)\rangle = |ll\rangle \cos(\varphi/2) + |\phi^+\rangle \sin(\varphi/2)$, where $\tan\varphi = \sqrt{2}B_x/(1 - |B_z|)$. When $B_z > 0$, $|ll\rangle = |11\rangle$; when $B_z < 0$, $|ll\rangle = |00\rangle$.

The coupling of this system to a probe qubit provides us with a natural way of measuring the phase transition. As before, we use an Ising-type interaction, which results in the total Hamiltonian

$$H = H_T^s + \varepsilon\sigma_z^0(\sigma_z^1 + \sigma_z^2). \tag{5}$$

To measure the QPT, we first initialize the system into the ground state $|\psi_g(B_x, B_z)\rangle$ in a given longitudinal field B_z. As we turn on the coupling to the probe qubit initially in $|+\rangle$, the combined system splits into two subsystems, corresponding to the two eigenstates of the probe qubit. In the two subsystems, the effective longitudinal field acting on qubits 1 and 2 is $1 - |B_z| \pm \varepsilon$, i.e. the coupling shifts the two subsystems in opposite directions along the B_z-axis. The eigenstates of the two subsystems are therefore also different. In terms of the mixing angle φ, the sensitivity of the basis states to the variation of the longitudinal field can be quantified as

$$d\varphi/d|B_z| = \sqrt{2}B_x/[2B_x^2 + (1 - |B_z|)^2]. \tag{6}$$

Apparently, this is a resonant effect: The sensitivity reaches a maximum at the QPT and falls off with the distance from the critical points like a Lorentzian. The full width of this "resonance line" is equal to the splitting $2\sqrt{2}B_x$ of the two lowest energy levels at the critical point.

To measure this behavior, we initialize the probe qubit into the $|+\rangle$ state. As we turn on the coupling to the system, each subsystem is no longer in an eigenstate, but starts to evolve in its new basis. The initial state $|+\rangle|\psi_g(B_x, B_z)\rangle$ evolves as

$$|\Psi(\tau)\rangle = [|0\rangle|\Psi_0(\tau)\rangle + |1\rangle|\Psi_1(\tau)\rangle]/\sqrt{2}. \tag{7}$$

Here $|\Psi_0(\tau)\rangle$ describes the two system qubits coupled to the state $|0\rangle$ of the probe qubit, evolving under the Hamiltonian $H_0 = H_T^s + \varepsilon(\sigma_z^1 + \sigma_z^2)$. Similarly, $|\Psi_1(\tau)\rangle$ describes the probe qubit in state $|1\rangle$ and evolves under $H_1 = H_T^s - \varepsilon(\sigma_z^1 + \sigma_z^2)$. We use this differential evolution for measuring the QPT via the overlap $L = |\langle\Psi_0(\tau)|\Psi_1(\tau)\rangle|^2$.

Figure 4 shows the quantum circuit and pulse sequence that implement this measurement. The initialization section prepares $|+\rangle|\psi_g(B_x, B_z)\rangle$, and the probing section implements the global evolution $U(\tau)$ approximately by decomposing it into $e^{-i\tau B_x(\sigma_x^1+\sigma_x^2)/2}e^{-i\tau\sigma_z^1\sigma_z^2}e^{-i\tau\varepsilon\sigma_z^0\sigma_z^1}e^{-i\tau\varepsilon\sigma_z^0\sigma_z^2}e^{-i\tau B_z(\sigma_z^1+\sigma_z^2)}e^{-i\tau B_x(\sigma_x^1+\sigma_x^2)/2}$. In the experiments, we measured the overlap L for a transverse field strength of $B_x = 0.1$, coupling strengths of $\varepsilon = 0.2$ and 0.3, and a range of longitudinal fields, $-2 \leq B_z \leq 2$. The evolution time was set to $\tau = 1.6$. The approximations used in the implementation of $U(\tau)$ reduce the fidelity by less than 1.4%.

The experimental results are shown as Figure 5, where the experimentally measured overlaps L are marked by "*" and "×" for $\varepsilon = 0.2$ and 0.3, respectively. The experimental data are fitted to aL_0, where L_0 denotes the corresponding theoretical result. The best agreement was obtained for $a = 0.84$ and 0.77, respectively; the corresponding functions are shown as the dark and light curves. Obviously the critical points are correctly identified by the minima of L, indicating increased sensitivity of the ground state to the perturbation by the probe qubit. The differences between the theoretical and experimental values are mainly caused by imperfections of the radio frequency pulses, inhomogeneities of magnetic fields and decoherence.

Discussion and Conclusion. — In conclusion, we have shown that a probe qubit can be used to detect quantum critical points. It is first placed into a superposition state and then coupled to the system undergoing the QPT. When the two eigenstates become correlated to two different phases, the superposition decoheres. The loss of coherence is thus a direct measure of the QPT.

We have applied this procedure to two types of QPTs, choosing the couplings between the probe and the system in such a way that the two states of the probe induce slightly different values of the control parameter [12, 17]. No details have to be known about the phases on the two sides of the phase transition. Only one qubit is measured for the detection of the critical points, independent of the size of the simulated quantum system. Hence this method scales very favorably with the size of the system [15, 18]. Theoretical results indicate that the overlap L remains a useful measure for larger systems in Ising and XY spin chains [12]. For the more complex quantum phase transitions where many states are close to the ground state (e. g. spin glass), our fidelity method seems to work, although the details are still being worked out [19].

In the present example, the probe qubit was coupled to all system qubits in a symmetric way. For other systems, the type of coupling required may depend on the system Hamiltonian and the nature of the phases on both sides of the QPT. While a full discussion of this issue is far beyond the scope of this letter, we expect that if the phase change involves delocalized states (e.g. spin waves), a single coupling between the probe qubit and one of the system qubits should be sufficient to detect the phase transition [20]. On the other hand, if the changes at the QPTs are local, a larger number of couplings or probe qubits may be required. In the extreme case, where critical points separate purely local changes, it may be necessary to couple the probe qubit to every system qubit or to implement couplings from a single probe qubit to all system qubits. Even in this worst case scenario, the number of probe qubits (or operations) only scales linearly with the size of the system; this should be contrasted to the readout by quantum state tomography, where the number of measurements increases exponentially with the system size. In future work, we plan to apply this type of analysis to the study of different types of phase transition, including quantum chaos [21]. Furthermore, it should be possible to use this approach for the characterization of decoherence [17] and errors that occur during quantum information processing [22].

---

[1] S. Sachdev, *Quantum Phase Transitions* (Cambridge University Press, Cambridge, 2000); M. Vojta, Rep. Prog. Phys. **66**, 2069 (2003); P. Coleman and A. J. Schofield, Nature (London) **433**, 226 (2005).

[2] J. Bardeen, L. N. Cooper, and J. R. Schrieffer, Phys. Rev. **108**, 1175 (1957).

[3] R. B. Laughlin, Phys. Rev. Lett. **50**, 1395 (1983).

[4] J. Custers et al., Nature (London) **424**, 524 (2003); M. Neumann et al., Science **317**, 1356 (2007); P. Gegenwart et al., *ibid.* **315**, 969 (2007).

[5] A. Yeh et al., Nature (London) **419**, 459 (2002).

[6] M. Greiner et al., Nature (London) **415**, 39 (2002); S. E. Sebastian et al., *ibid.* **441**, 617 (2006).

[7] A. Osterloh et al., Nature (London) **416**, 608 (2002).

[8] G. Vidal et al., Phys. Rev. Lett. **90**, 227902 (2003); M. C. Arnesen et al., *ibid.* **87**, 017901 (2001); R. Somma et al., Phys. Rev. A **70**, 042311 (2004).

[9] X. Peng el al., Phys. Rev. A **71**, 012307 (2005).

[10] I. L. Chuang et al., Proc. R. Soc. London, Ser. A **454**, 447 (1998).

[11] T. Gorin et al., Phys. Rep. **435**, 33 (2006).

[12] H. T. Quan et al., Phys. Rev. Lett. **96**, 140604 (2006); Z.-G. Yuan et al., Phys. Rev. A **75**, 012102 (2007).

[13] P. Zanardi et al., Phys. Rev. E **74**, 031123 (2006).

[14] A. J. Leggett, in *Fundamentals of Quantum Information*, Lecture Notes in Physics, Vol. 587 (Springer-Verlag, Berlin 2002), p.3.

[15] R. Somma et al., Phys. Rev. A **65**, 042323 (2002).

[16] D. G. Cory et al., Physica D **120**, 82 (1998); X. Peng et al., arXiv: quant-ph/0202010.

[17] F. M. Cucchietti et al., Phys. Rev. A **75**, 032337 (2007).

[18] R. Somma, G. Ortiz, E. Knill, J. Gubernatis, arXiv:quant-ph/0304063v1.

[19] F. M. Cucchietti (private communication).

[20] D. Rossini et al., Phys. Rev. A **75**, 032333 (2007).

[21] C. A. Ryan et al., Phys. Rev. Lett. **95**, 250502 (2005); J. Emerson et al., *ibid.* **89**, 284102 (2002).
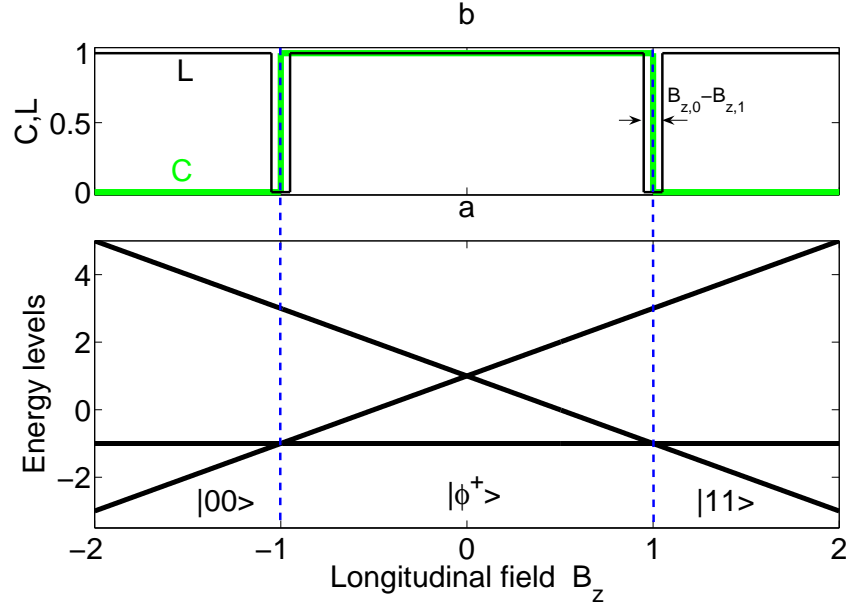
[22] B. Levi et al., Phys. Rev. A **75**, 022314 (2007).

FIG. 1: (Color online) (a) The energy levels of the system. (b) Concurrence (thick line) and overlap L (thin) of the ground state.
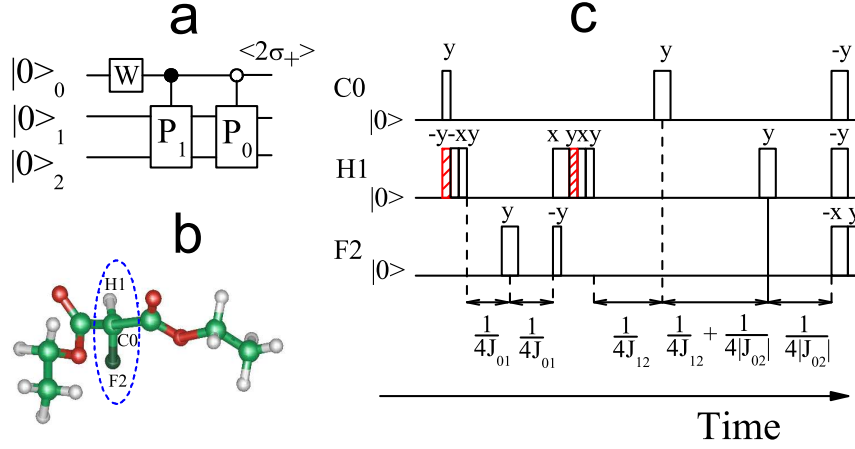
FIG. 2: (a) Quantum network for measuring L. W denotes the Walsh-Hadamard transform, and $\sigma_+ = (\sigma_x + i\sigma_y)/2$. The controlled operations P_0 and P_1 denote the evolutions for preparing $|\psi_g(B_{z,0})\rangle$ and $|\psi_g(B_{z,1})\rangle$, if qubit 0 is in state $|0\rangle$ or $|1\rangle$, respectively. (b) Chemical structure of Diethyl fluoromalonate. The three qubits are marked by the dashed oval. (c) Pulse sequence for measuring the state overlap. The narrow unfilled rectangles denote $\pi/2$ pulses, and the wide ones denote π pulses. The striped rectangles denote $\pi/4$ pulses. The directions along which the pulses are applied are denoted by $\pm x$ and $\pm y$. The durations of the pulses are so short that they can be ignored.
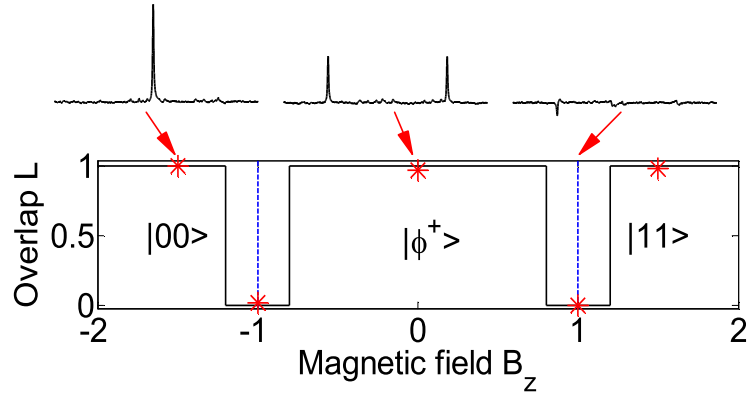
FIG. 3: Theoretical (line) and measured (asterisks) overlap L for the level-crossing case. Three NMR spectra illustrate the signals corresponding to $B_z = -1.5$, 0, and $+1$, respectively.
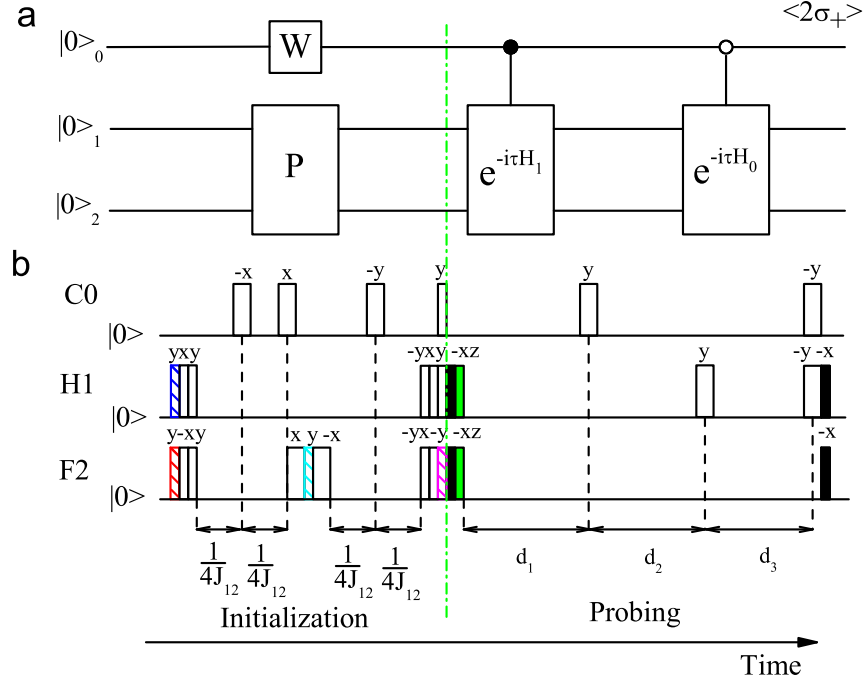
FIG. 4: (Color online) Quantum circuit (a) and pulse sequence (b) for measuring the overlap L for the avoided level-crossing case. P denotes the preparation of $|+\rangle|\psi_g(B_x, B_z)\rangle$ from $|000\rangle$. In the initialization section, the width of the filled pulse applied to H1 is $\theta - \frac{\pi}{2}$, and the width of the filled pulses applied to F2, from left to right, are $(\pi - \alpha)/2$, $(\alpha - \beta)/2$, and $(\pi - \beta)/2$, respectively, with $\tan(\alpha/2) = -\sqrt{2}c_1/c_+$, $\tan(\beta/2) = -c_+/\sqrt{2}c_0$, $\tan(\theta/2) = \sin(\beta/2)/\cos(\alpha/2)$. c_0, c_+ and c_1 denote the amplitudes of $|00\rangle$, $|\phi^+\rangle$ and $|11\rangle$ in $|\psi_g(B_x, B_z)\rangle$. In the probing section, the rectangles filled by heavy and light color denote the pulses with width τB_x and $2\tau B_z$, respectively, and $d_1 = \frac{\tau}{\pi}(\frac{\varepsilon}{J_{01}} + \frac{1}{J_{12}})$, $d_2 = \frac{\tau}{\pi}(\frac{\varepsilon}{|J_{02}|} + \frac{1}{J_{12}})$, and $d_3 = \frac{\tau\varepsilon}{\pi}(\frac{1}{J_{01}} + \frac{1}{|J_{02}|})$.
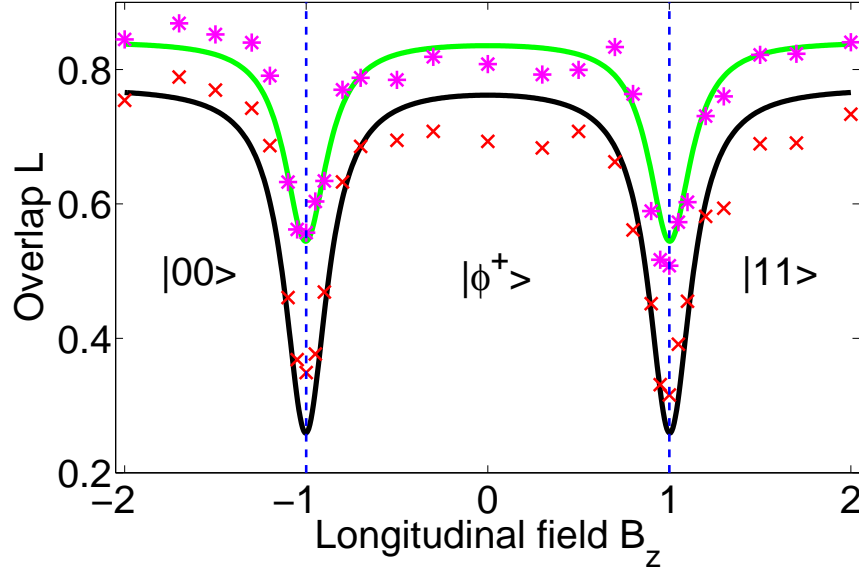
FIG. 5: (Color online) Experimental overlap L for $\varepsilon = 0.2$ marked by "*" and $\varepsilon = 0.3$ marked by "×". The experimental data are fitted to aL_0, and yielded $a = 0.84$ and 0.77, respectively, shown as the dark and light curves, where L_0 denotes the corresponding theoretical result.